Available online at www.sciencedirect.com
SCIENCE DIRECT
Polymer 46 (2005) 11416–11423
polymer
www.elsevier.com/locate/polymer

Temperature dependent elastic–plastic behaviour of polystyrene studied using AFM force–distance curves

Senthil Kumar Kaliappan, Brunero Cappella *

Laboratory VI.21, Federal Institute for Materials Research and Testing (BAM), Unter den Eichen 87, D-12205 Berlin, Germany

Received 7 June 2005; received in revised form 19 September 2005; accepted 21 September 2005
Available online 19 October 2005

Abstract

Force–displacement curves have been obtained on two polystyrene samples, having different molecular weight, at various temperatures and probe rates using an atomic force microscope. The force–displacement curves have been analysed using a novel method, which extends continuum elastic contact theories also to the plastic deformations. The Young's modulus and the yielding force of the two polystyrene samples have been determined as a function of temperature and frequency. It was also possible to calculate the Williams–Landel–Ferry coefficients for measurements above the glass transition temperature, and the viscoelastic activation energy for measurements below the glass transition temperature using the Arrhenius equation. All the calculated coefficients were in very good agreement with the literature values. The measured quantities span a wide range of temperature (85 °C) and frequency (eight decades) and the shifts of all the quantities calculated from force–displacement curves obey the Williams–Landel–Ferry and Arrhenius equation with the same parameters. Quantitative and qualitative comparison of the Young's modulus, of the stiffness in the plastic region and of the yielding force of the two polystyrene samples revealed different viscoelastic behaviour because of the variation in glass transition temperature of the two samples, due to their difference in the molecular weight.

Keywords: Force–displacement curves; Viscoelastic properties; Time–temperature superposition

1. Introduction

Atomic force microscope (AFM) force–displacement curves are useful in determining the elastic properties of polymers [1–5]. Of late, the focus of the research work has been shifted to the determination of the glass transition temperature T_g using force–displacement curves [6–8]. At T_g changes occur in the local movement of polymer chains that lead to large variations in a host of physical properties. Hence, by studying T_g much can be revealed about the relationship between structure and properties of amorphous polymers. Some physical properties that vary at T_g include density, specific heat, elastic modulus, dielectric and acoustical properties, and rate of gas or liquid diffusion through the polymer. Any of these properties can be used to determine the T_g. For example, around T_g there is about three orders of magnitude decrease in the elastic modulus of the polymers. As AFM is a powerful tool to study the local properties of materials with high lateral resolution, the study of the elastic properties of polymer systems around T_g with AFM gives the possibility to characterize complex structures, e.g. copolymers domains that cannot be examined with other techniques.

In the earlier works on determination of T_g using force–displacement curves [6–8], researchers have used primarily the work of adhesion as the quantity to determine T_g. In the work by Marti et al. [6], the authors observed a large increase in adhesion above a certain temperature depending on the molecular weight of polystyrene. Later, Tsui et al. [7] were able to draw an adhesion master curve using force–displacement curves. Finally, Bliznyuk et al. [8] were able to calculate from force–displacement curves several quantities, which change abruptly at $T=T_g$. However, except the pull-off force, all the other quantities measured do not reflect on any of the physical parameters describing the polymer. Hence, the experiment of Bliznyuk et al. was only a method to determine T_g without giving insights into the physical processes occurring around T_g.

Till date, there has been very little theoretical and experimental works done to study the plastic deformations and the yielding force of a polymer using force–displacement curves [5]. In our previous experiment on poly (*n*-butyl methacrylate) (PnBMA) [9], it was possible to determine

* Corresponding author. Tel.: +49 30 8104 3343.
E-mail address: brunero.cappella@bam.de (B. Cappella).

0032-3861/$ - see front matter © 2005 Elsevier Ltd. All rights reserved.
doi:10.1016/j.polymer.2005.09.066

the modulus of PnBMA as a function of temperature and probe time using a novel model for analysis based on Hertz theory [10] and time-temperature superposition principle. With this model, it was not only possible to calculate the elastic modulus of PnBMA, but also the stiffness in the plastic regime and the yielding force of PnBMA as a function of temperature and probe rate. The results obtained using AFM force–displacement curves were in good agreement with the values obtained using two other techniques, namely dynamic mechanical analysis (DMA) and broadband spectroscopy.

The T_g of a homopolymer generally increases up to a limiting value, known as the limiting or persistent T_g value, with increase in molecular weight, but the reverse may hold for polymers with functionalised end-groups, or where crystallinity decreases with increasing molecular weight [11]. The increase of T_g with molecular weight has been generally understood as the effect of increasing number of polymer chain entanglements. Fox–Flory relation [12] describes the dependency of glass transition temperature of a polymer on its molecular weight:

$$T_g = T_{g,\infty} - \frac{K}{M_n} \quad (1)$$

where $T_{g,\infty}$ is the glass transition temperature of the polymer with infinite molecular weight, K is an empirical constant and M_n is the number average molecular weight. For polystyrene is $T_{g,\infty} = 100$ °C and $K = 1.8 \times 10^5$ °C. At small M_n, there is a large increase in T_g for small increases in M_n, but for large M_n there is no significant increase in T_g with increasing M_n. The number average molecular weight at which there is no further significant increase in T_g with increasing M_n is called the critical molecular weight. Below the critical molecular weight a large variation in T_g of the polymer is possible with respect to changes in M_n. Hence, the viscoelastic properties of a polymer depend also on the molecular weight.

In this article, we present force–displacement curves acquired on two polystyrene samples having different molecular weights at various temperatures and frequencies. The novel method of analysis permits us to characterise the Young's modulus, the stiffness in the plastic region, and the yield strength as functions of temperature and frequency for the two samples of different molecular weights.

2. Experimental section

Two different molecular weights of polystyrene (PS), namely 4.2 kDa (PS4K) and 62.5 kDa (PS62K) were purchased from Polymer Standards Service GmbH, Mainz, Germany. The glass transition temperatures are 57 and 97 °C, respectively. The polydispersity index is $M_w/M_n = 1.05$ for both polymer samples. The polymers were used without further purification. Concentrated polymer solutions in toluene were cast on to glass slides as films. The films were allowed to dry in air for 2 weeks. Prior to use, the films were annealed in a vacuum oven, for 1 week, at 150 °C. The resulting films were relatively thick (≈ 250 μm) allowing us to perform large indentations without undesirable artefacts due to the large stiffness of the substrate [13]. In order to avoid such artefacts, indentation depths should not exceed 10% of the film thickness [14].

AFM force–distance curves were acquired using a commercial MFP-3D microscope (Asylum Research, Santa Barbara, CA). Since the idea is to provoke plastic deformation, a rather stiff cantilever was used. Furthermore, if the spring constant of the cantilever is less than the elastic modulus of the probed surface, then force–distance curves will basically measure the cantilever's stiffness [15]. If the cantilever's spring constant is too high, then the force resolution turns out to be bad. Hence, Ultrasharp cantilever (Mikro Masch, Estonia) having a spring constant of $k_c = 15$ N/m was used to acquire all the force–distance curves. The spring constant has been measured from the noise spectrum of the cantilever [15].

A miniature metal plate at the basis of the polymer was heated using a 340-temperature controller (Lake Shore Cryotronics, Westerville, OH) and the surface temperature was measured directly using a PT100 fixed on to the polymer surface. The temperature was allowed to equilibrate overnight at each experimental temperature, which stayed constant ($\pm$ 0.3 °C on the surface) for several days. Force–displacement curves were obtained at various temperatures for PS4K (from 30 to 95 °C over 42, 54, 61, 67, 75, and 82 °C) and for PS62K (from 30 to 84 °C over 41, 52, and 62 °C). At every experimental temperature force–displacement curves have been obtained at various frequencies (usually 30, 10, 1, 0.5, 0.1, and 0.03 Hz) with high sampling density for better resolution of the curves. Since the minimum step of the vertical piezo displacement is 1 pm and the piezoactuator acts like a capacitor, the piezoactuator displacement has been assumed to be continuous, and the probe rate is the frequency of the piezoactuator displacement, i.e. the frequency of the force–displacement curve.

For each measurement at a particular temperature and frequency, a variable number of force–displacement curves have been obtained (from 100 up to 300). Each set of 100 force–displacement curves was acquired at different areas of the samples (usually 20×20 μm^2) in force volume acquisition mode. Small variations in the sample topography allowed the acquisition of force–displacement curves with varying indentation depths. In total, more than ca. 15,000 curves have been taken into account for the analysis.

3. Results and discussion

The force–displacement curves in Fig. 1(a) have been obtained at various temperatures and frequencies on PS4K (from left to right: 30 °C at 30 Hz, 42 °C at 0.1 Hz, 61 °C at 0.1 Hz, 75 °C at 0.1 Hz, 82 °C at 0.1 Hz and 95 °C at 1 Hz) and on PS62K in Fig. 1(b) (from left to right: 30 °C at 1 Hz, 41 °C at 0.03 Hz, 52 °C at 0.1 Hz, 62 °C at 0.1 Hz and 84 °C at 1 Hz). For clarity, only the withdrawal contact lines of the force–displacement curves acquired on PS4K at 30 °C and 30 Hz, and at 75 °C and 0.1 Hz are shown in Fig. 1(a). The piezo displacement axis measures the position of the tip with respect to the sample surface, where negative displacements

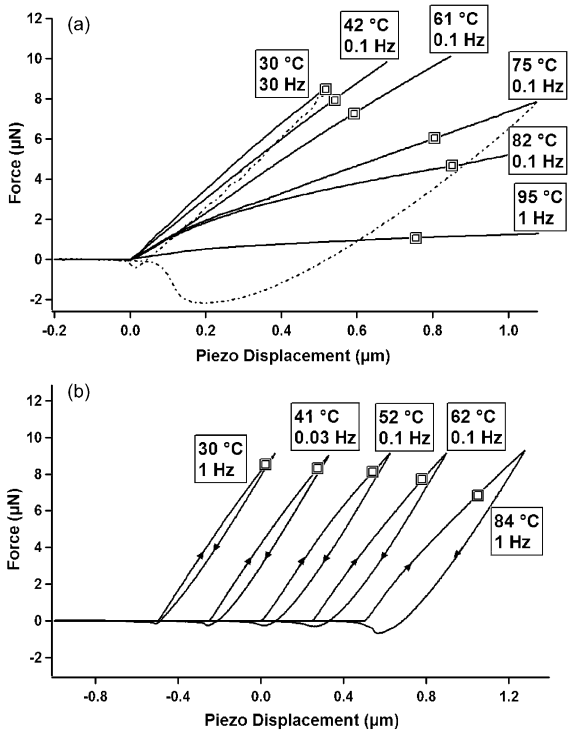

Fig. 1. Approach contact lines (solid lines) and withdrawal contact lines (broken lines) of the force–displacement curves acquired on PS4K at various temperatures and frequencies are shown in Fig. 1(a). From left to right: 30 °C at 30 Hz, 42 °C at 0.1 Hz, 61 °C at 0.1 Hz, 75 °C at 0.1 Hz, 82 °C at 0.1 Hz and 95 °C at 1 Hz. Only the withdrawal contact lines acquired at 30 °C and 30 Hz and at 75 °C and 0.1 Hz are represented for clarity. Force–displacement curves acquired on PS62K at various temperatures and frequencies are shown in Fig. 1(b). From left to right: 30 °C at 1 Hz, 41 °C at 0.03 Hz, 52 °C at 0.1 Hz, 62 °C at 0.1 Hz and 84 °C at 1 Hz. The force–displacement curves have been shifted horizontally for clarity (the curve at 52 °C and 0.1 Hz is the reference). Upward (downward) arrows represent the approach (withdrawal) contact lines. The yielding points are marked using double-bordered squares.

correspond to movements of the tip away from the sample surface and positive displacements correspond to movements of the tip into the sample and thereby indenting the sample. The tip deflection due to the interaction with the sample can be measured with an optical lever deflection system and the applied force can be calculated, provided the spring constant of the cantilever is already known. The sample deformation D along the contact line is given by:

$$D = Z - \delta_c \tag{2}$$

where Z is the piezo displacement and δ_c is the cantilever deflection. The first derivative of the approach contact line is the stiffness of the sample. Hence, by observing the changes in the first derivative, it is possible to infer the variations in sample stiffness due to changes in one or more experimental parameters such as temperature or frequency [15,16].

Some of the features of the force–displacement curves can be immediately pointed from Fig. 1(a). The curves acquired on PS4K present yielding points [17], which are represented in Fig. 1(a) as double-bordered squares. The yielding force is a critical force $F_{yield} = k_c \delta_{yield}$, at which the polymer starts to undergo plastic deformations and the sample stiffness starts to decrease. The yielding point can be seen as a kink in the approach contact line of a force–displacement curve. Looking at the force–displacement curves acquired on PS4K, the effect of temperature and frequency on the yielding point is quite evident. The yielding force decreases with increase in temperature and/or probe time and the first derivative of the approach contact line decreases with increase in temperature and/or probe time both before and after the yielding point. This implies that the polymer becomes softer, both in the elastic and in the plastic regime of deformations, as the temperature increases. Besides the variation in the first derivative of the approach contact line, variation in yielding force is also a good indicator to predict whether the polymer surface is below or above its T_g, while above T_g there is a remarkable decrease in the yielding force with respect to increase in temperature and/or probe time. It can be noted that for the curves acquired at 30 and 42 °C there is no distinguishable decrease in the yielding force and only a small decrease in stiffness with increase in temperature and/or probe time.

The force–displacement curves acquired on PS62K are shown in Fig. 1(b). The curves have been shifted horizontally for clarity. The changes in the first derivative of the approach contact line of the force displacement curves cannot be easily observed as in the case of PS4K. Hence, the increase in temperature and/or probe time has no pronounced effects on the stiffness of PS62K in the experimental temperature range. Also, the yielding force almost remains a constant, irrespective of the probe temperature and frequency.

The comparison of the approach contact lines of the two samples with different molecular weights reveals that PS4K has more pronounced changes in the first derivative of the approach contact line and hence that the stiffness of PS4K varies more than that of PS62K in the used experimental temperature range. Also, the decrease in yielding force with increase in temperature and/or probe time is far greater in case of PS4K when compared with PS62K, where the yielding force almost remains a constant at any temperature and/or probe time. These differences in stiffness and yielding force between PS4K and PS62K are due to their respective glass transition temperatures, which in turn depend on their molecular weights. In case of PS4K, the stiffness starts to decrease around T_g (57 °C), where the polymer is in the glass–rubber transition state, whereas PS62K is in its glassy state over the entire experimental temperature range.

Considering the withdrawal contact lines acquired on PS62K in Fig. 1(b), it can be noted that the approach and the withdrawal curves do not overlap each other. This is due to the presence of plastic deformations, as confirmed by the presence of a yielding point. During the withdrawal of the tip, the sample cannot regain its original shape and the force exerted by the cantilever at every indentation depth is smaller than during the approach of the tip [1,18–20]. The non-overlapping behaviour of the approach and withdrawal contact lines is called hysteresis of the force–displacement curves. The energy that has been transferred by the tip to the sample during the approach contact phase is not completely transferred back to the tip during the withdrawal contact phase. We can define

the permanent plastic deformation D_p as the intercept of the withdrawal contact line with the axis $F=0$ and the area between the approach and the withdrawal contact lines above the zero axis as the energy dissipated in the sample.

As it can be seen from Fig. 1(b), the hysteresis and the permanent plastic deformation increase slowly with increase in temperature and/or probe time. In case of the withdrawal contact lines of PS4K in Fig. 1(a), there is a large increase in hysteresis with increasing temperature and/or probe time. The reason for this large increase in the hysteresis with increasing temperature and/or probe time can be attributed to the fact that PS4K is softer than PS62K at high temperatures in our experimental temperature range. At high temperatures PS4K is in the transition from glass to rubber state, whereas PS62K is still in the glassy state. The permanent plastic deformation for a certain maximum force can be effectively used to compare the hardness of the two polymers. For example, the permanent plastic deformation of PS4K at 82 °C and 0.1 Hz is about 600 nm, whereas the permanent plastic deformation of PS62K at 84 °C and 1 Hz is only about 200 nm. This confirms that the high molecular weight polymer PS62K remains harder than the low molecular weight polymer PS4K at high temperatures in our experimental temperature range. The difference in hardness at a certain temperature is in turn due to the difference in molecular weights and glass transition temperatures.

It is important to note that the stiffness and yielding force do not depend on the maximum applied force, i.e. all approach curves at a certain temperature and frequency overlap each other independent of the maximum force. However, this is not the case with withdrawal curves, where the plastic deformation and work of adhesion depend on the maximum applied force.

The effect of temperature and frequency on the yielding force and stiffness can be quantitatively determined [9]. The model used for analysis has been exhaustively described in the above-cited article, hence only the important findings are described in this article. The basic idea behind this model is to describe the elastic deformation and the plastic deformation, which is treated as an elastic deformation with smaller stiffness, using the Hertz theory [10]. According to the Hertz theory the applied force and the sample deformation are related as

$$F = k_c\delta_c = E_{tot}\sqrt{R}D^{3/2} = \frac{4}{3(1-\nu_s^2)}E\sqrt{R}D^{3/2} \Rightarrow$$
$$D^{3/2} = \frac{3(1-\nu_s^2)}{4}\frac{1}{E}\frac{k_c}{\sqrt{R}}\delta_c \quad (3)$$

where R is the tip radius, ν_s is the Poisson's ratio and E is the Young's modulus of the sample. E_{tot} is defined by:

$$\frac{1}{E_{tot}} = \frac{3}{4}\left(\frac{1-\nu_s^2}{E} + \frac{1-\nu_t^2}{E_t}\right) \quad (4)$$

where ν_t and E_t are the Poisson's ratio and Young's modulus of the tip. If E_t is much larger than E, we can write $E_{tot} = (4/3(1-\nu_s^2))E$. The proportionality between $D^{3/2}$ and the applied force is predicted by all other continuum contact theories, provided the forces are shifted by a factor depending on the adhesion between the tip and the sample [21]. When the adhesive force is much smaller than the applied force, the difference in the resulting Young's modulus becomes smaller and when modelling approach curves the effect of adhesion can be neglected [22]. It is important to remember that the elastic continuum theories may be applied only to the elastic part of the indentation curve, and not to the plastic part. Hence, when we speak of adhesion, we mean the adhesion measured in the curves where only elastic deformations take place, i.e. $F_{max} < F_{yield}$. In this case the adhesion is always much smaller than the maximum applied load (see Fig. 1(b), where the plastic deformations are very small and, at least at low temperatures, negligible).

The $D^{3/2}$ vs. cantilever deflection curve (open circles) shown in Fig. 2 presents two linear regions connected by another region. The two linear regions are the elastic and the plastic regimes of the deformation. The slope of the second region is always larger than that of the first region. From Eq. (3) it can be seen that the slope in the initial elastic region is inversely proportional to the Young's modulus of the sample. Hence, any increase in slope corresponds to a decrease in the stiffness of the sample, which is the expected behaviour at $\delta_c = \delta_{yield}$. The non-linear region connecting the elastic and the plastic regions is the result of a distribution of yielding points.

$D^{3/2}$ curves have been fitted with a hyperbola in the form [9]:

$$y = D^{3/2}(\delta_c) = (\beta\delta_c - \varepsilon) + \sqrt{\alpha^2\delta_c^2 - 2\varepsilon(\beta-\gamma)\delta_c + \varepsilon^2} \quad (5)$$

with $\alpha>0$, $\beta>0$, $\gamma>0$, $\varepsilon>0$, and $\beta-\alpha<\gamma<\beta+\alpha$.

In the two linear regions where $D^{3/2}$ is proportional to δ_c the hyperbola can be approximated with two lines, i.e. its tangent

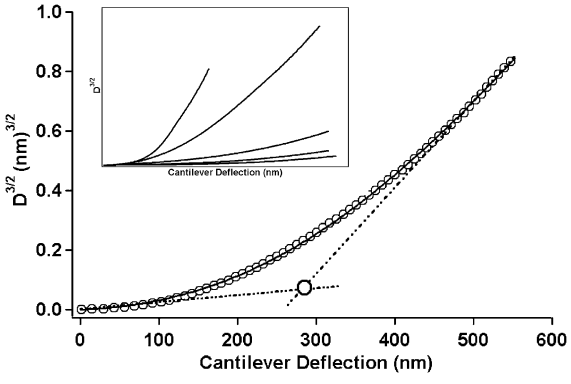

Fig. 2. Calculated average $D^{3/2}$ curve (open circles) at 75 °C and 0.1 Hz versus the cantilever deflection and the hyperbolic fit (solid line) on PS4K. The two linear regimes are represented as dotted lines and the intersection of these lines provides the yielding point δ_{yield}. Inset shows the calculated average $D^{3/2}$ functions at various temperatures and frequencies. From right to left: 30 °C at 30 Hz, 42 °C at 0.1 Hz, 61 °C at 0.1 Hz, 75 °C at 0.1 Hz and 82 °C at 0.1 Hz.

at $\delta_c = 0$ and its asymptote for $\delta_c \to \infty$, respectively:

$$\begin{cases} \delta_c \ll \delta_{yield} \Rightarrow y \cong y'(0)\delta_c \Rightarrow D^{3/2} \cong \gamma\delta_c \\ \delta_c \gg \delta_{yield} \Rightarrow y \cong \left(\lim_{\delta_c \to \infty} y'\right)\delta_c + \lim_{\delta_c \to \infty}(y - \delta_c y') \Rightarrow \\ D^{3/2} \cong (\beta + \alpha)\left[\delta_c - \frac{\varepsilon}{\alpha}\left(1 - \frac{\gamma}{\alpha + \beta}\right)\right] \end{cases} \tag{6}$$

and δ_{yield} can be defined as the intersection of the two lines, given by:

$$\delta_{yield} = \frac{\varepsilon}{\alpha} \tag{7}$$

It is important to note that this model treats the yielding region as a transition from the first elastic deformation to a second deformation with a lower stiffness. Thus, a plastically deformed polymer can be treated, only from a mathematical point of view, as an elastically deformed polymer with a smaller stiffness, by changing the origin of the $D^{3/2}$ vs. δ_c plots from the point [0,0] to the point [δ_{yield}, $D^{3/2}(\delta_{yield})$].

Fig. 2 shows the average $D^{3/2}$ calculated from 100 curves obtained at 75 °C and 0.1 Hz versus the cantilever deflection δ_c on PS4K and the inset shows the calculated $D^{3/2}$ curves (from right to left) at 30 °C and 30 Hz, 42 °C and 0.1 Hz, 61 °C and 0.1 Hz, 75 °C and 0.1 Hz and 82 °C and 0.1 Hz on PS4K. The yielding point (circle) calculated from the $D^{3/2}$ curve at 75 °C and 0.1 Hz is the intersection of the two lines. The effect of temperature on the $D^{3/2}$ curves can be seen from the inset. In case of PS4K the slope in the elastic regime, i.e. the first linear regime, increases with increase in temperature and/or probe time. Though there is a noticeable increase in the slope of the first linear regime of the $D^{3/2}$ curves with an increase in temperature, the increase in the slope of the second linear regime of the $D^{3/2}$ curves is even more pronounced, implying larger decrease in the stiffness after yielding. In comparison the $D^{3/2}$ curves calculated from the curves acquired on PS62K show very little changes in the slope of the two linear regimes with increase in temperature. Hence, the decrease in stiffness of the higher molecular weight PS62K is smaller in comparison to the decrease in stiffness of the lower molecular weight PS4K with increasing temperature because of their different glass transition temperatures.

All the average $D^{3/2}$ curves obtained at different temperatures and frequencies have been fitted with a hyperbola. Thus the parameters describing the elastic–plastic behaviour of the polymers, i.e. $\alpha+\beta$, γ, and δ_{yield}, are obtained as a function of temperature and frequency. Isotherms of these calculated parameters, which are the curves describing the effect of frequency at a particular temperature, are plotted. Taking advantage of time-temperature superposition principle (TTS) the measured isotherms can be shifted horizontally to obtain the master curve for each measured quantity. In TTS, the effect of a shift of temperature is equivalent to a certain shift of frequency for most of the physical properties of the polymers. The reference temperature T_{ref} has been chosen to be 54 and 84 °C, for PS4K and PS62K, respectively. Every isotherm has been shifted till it overlaps the isotherm obtained at the reference temperature. A shift to the left corresponds to an increase of the frequency and hence a decrease of the temperature. The overlapping isotherms result in the master curve (filled circles in Fig. 3) of the measured property as a function of frequency or equivalently temperature. Fig. 3 shows the master curve obtained for the quantity $[3(1-\nu_s^2)/4][1/(\alpha+\beta)] = 0.67/(\alpha+\beta)$ as a function of log(ν) for PS4K sample. The Poisson's coefficient ν_s of the sample has been assumed to be 0.33, which is a common value found for polymers. The quantity $0.67/(\alpha+\beta)$ is proportional to the stiffness of the polymer in the plastic regime.

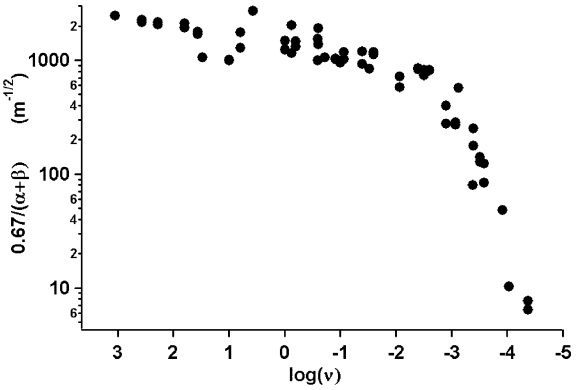

Fig. 3. Master curve of the calculated parameter $0.67/(\alpha+\beta)$, which is proportional to the stiffness after yielding, as a function of log(ν). The master curve has been obtained by shifting horizontally the isotherms of the considered parameter by a shift factor log a_T till they overlap the reference isotherm at 54 °C.

The Williams–Landel–Ferry (WLF) equation [23] is suitable to describe the relation between the shift coefficients log a_T and the temperature in the temperature range T_g to T_g + 100 °C. The WLF equation is:

$$\log a_T = \frac{-C_1(T - T_{ref})}{C_2 + (T - T_{ref})} \tag{8}$$

where C_1 and C_2 are constants. Since the T_g of PS4K and PS62K are 57 and 97 °C, respectively, Arrhenius equation is also needed in order to equate temperature and frequency for the measurements done below the glass transition temperature. The Arrhenius equation is:

$$\ln a_T = \frac{E_a}{R}\left(\frac{1}{T} - \frac{1}{T_{ref}}\right) \tag{9}$$

where E_a is the viscoelastic activation energy of the polymer, R is the universal gas constant (8.3144×10^{-3} kJ/mol K) and T_{ref} is the reference temperature.

In case of PS62K, all measurements were performed below the glass transition temperature of the polymer and hence only Arrhenius equation was used to fit the shift coefficients. For PS4K, some measurements were done below T_g (30 and 42 °C) and the other measurements were done above T_g (61, 67, 75, 82 and 95 °C), hence both WLF and Arrhenius equation were used to fit the shift coefficients. Fig. 4 shows the shift coefficients vs.

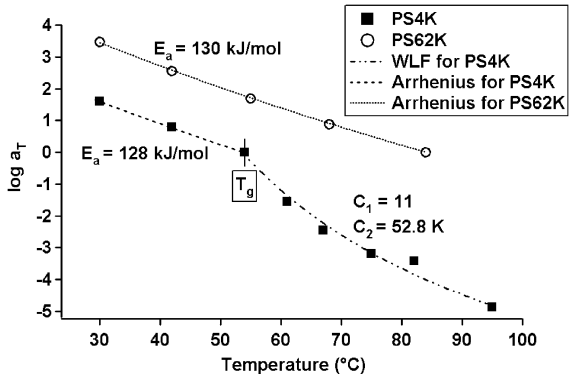

Fig. 4. Shift coefficients log n a_T, used in obtaining the master curve from isotherms, as a function of temperature for PS4K (filled squares) and PS62K (open circles). The reference temperature is 54 and 84 °C for PS4K and PS62K, respectively. The fits of the shift coefficients have been calculated using Arrhenius equation and WLF equation. The activation energy E_a has been calculated from the measurements done below T_g as 128 and 130 kJ/mol for PS4K and PS62K, respectively, using the Arrhenius equation. The constants C_1 and C_2 have been determined from the measurements done above T_g for PS4K as 11 and 52.8 K, using WLF equation. It can be seen that for PS4K, the transition from Arrhenius to WLF fit is unambiguous. The intersection of the two fits gives the T_g of PS4K.

temperature for PS4K and PS62K and the corresponding fits using WLF and Arrhenius equations. In case of PS4K, there is a rather definite transition from the Arrhenius fit to the WLF in the vicinity of $T=54$ °C. Hence, the intersection of the Arrhenius and the WLF fit yields an estimation of T_g, which is in good agreement with the expected value for PS4K ($T_g=$ 57 °C). The parameters calculated from the fits of the shift coefficients are $C_1=11$ and $C_2=52.8$ K, and $E_a=128$ kJ/mol for PS4K and $E_a=130$ kJ/mol for PS62K. All the fit parameters measured using force–displacement curves, especially γ and δ_{yield}, obey the Williams–Landel–Ferry equation and Arrhenius equation with the same constants.

The constants C_1 and C_2 are in good agreement with the literature values. Results from dynamic mechanical studies of polystyrene have shown evidence for three sub-T_g transitions for polystyrene. These include β (ca. 325 K), γ (ca. 130–180 K), and δ (ca. 30–40 K) transitions with activation energies of about 147, 42 and 8–13 kJ/mol, respectively [24]. The δ relaxation has been associated with hindered partial rotation and wagging of the phenyl group [25]. The origin of the γ transition is less certain and may be due to the motion of the end groups. The results of molecular dynamics simulations suggest that the β relaxation may include crankshaft type motions of the PS backbone and librational motions of the pendant phenyl rings that depend upon the local environment [26]. The calculated viscoelastic activation energy for two samples is in good agreement with the literature value for β relaxation occurring at 52 °C, which is within the experimental temperature range. Thus, the novel analysis method together with TTS is effective in estimating the activation energy required for the β relaxation process to occur in polystyrene.

The Young's modulus of the sample can be calculated from the parameter γ and the analogue of the Young's modulus in the plastic deformation region from the parameter $\alpha+\beta$. Following the Hertz theory, for $\delta_c \ll \delta_{yield}$:

$$D^{3/2} \cong \gamma\delta_c \Rightarrow E \cong \frac{3(1-\nu_s^2)}{4}\,\frac{k_c}{\sqrt{R}}\,\frac{1}{\gamma} \tag{10}$$

and for $\delta_c \gg \delta_{yield}$:

$$D^{3/2} = (\alpha+\beta)\left[\delta_c - \left(1-\frac{\gamma}{\alpha+\beta}\right)\delta_{yield}\right] \Rightarrow D^{3/2} - \gamma\delta_{yield}$$
$$= (\alpha+\beta)(\delta_c - \delta_{yield}) \Rightarrow \bar{E} = \frac{3(1-\nu_s^2)}{4}\,\frac{k_c}{\sqrt{R}}\,\frac{1}{(\alpha+\beta)} \tag{11}$$

$\bar{E}$ is the proportionality factor between the additional deformation $D^{3/2}-\gamma\delta_{yield}$ and the 'reduced' force $F=k_c(\delta_c-\delta_{yield})$ during the plastic deformation. This parameter $\bar{E}$ can be seen, only from a mathematical point of view, as the analogue of the Young's modulus in the plastic deformation region. Fig. 5(a) shows the Young's modulus E and Fig. 5(b) the analogue of the Young's modulus for plastic deformations $\bar{E}$ of PS4K and PS62K in logarithmic scale as a function of temperature. The elastic moduli of the two polystyrene samples with different molecular weights as a function of temperature and frequency have been measured for the first time using AFM force–displacement curves. Thanks to WLF and Arrhenius equation, the temperatures can be calculated from the probe frequencies using the constants obtained from Eqs. (8) and (9). In calculating the Young's modulus, knowledge of

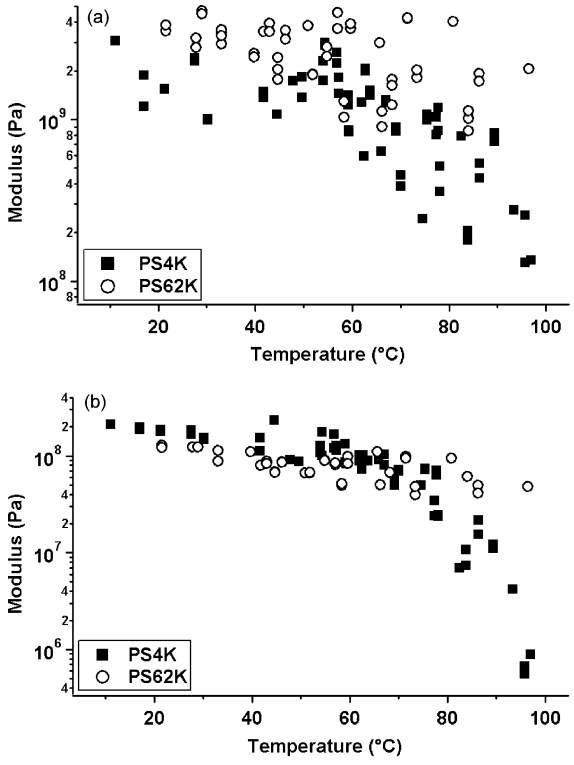

Fig. 5. Young's modulus E (5a) and its analogue for plastic deformations (5b) of PS4K (filled squares) and PS62K (open circles), calculated using Eqs. (10) and (11), as a function of temperature.

exact spring constant of the cantilever and of the tip radius is important. The spring constant has been measured from the noise spectrum of the cantilever [15] and is $k_c = 15$ N/m. The tip radius has not been measured, rather it has been chosen so that the AFM data match the expected Young's modulus value of PS around room temperature ($E = 2$–4 GPa). For $R = 20$ nm there is a good agreement with the expected value. Although such a value of the tip radius is only a rough approximation, it compensates some of the errors due to approximation of the tip as a Hertzian spherical tip.

The Young's modulus is an important parameter describing the mechanical properties of a polymer and it decreases almost three orders of magnitude around T_g. From Fig. 5(a) it can be seen that the Young's modulus of PS4K starts to decrease around $T_g \approx 57$ °C. The Young's modulus of PS4K in its glassy state is ≈ 3 GPa around 10 °C (about 50 °C below T_g) and then starts to decrease around T_g and reaches a value of ≈ 130 MPa around 100 °C (about 45 °C above T_g) in the glass–rubber transition state. Hence, we are able to see more than a decade decrease in the Young's modulus of PS4K as the temperature increases. In comparison, the modulus of PS62K remains nearly constant throughout the entire range of experimental temperature. The modulus of PS62K is 3.5 GPa around 20 °C (about 75 °C below T_g) and is 2 GPa around 100 °C (about T_g). On quantitatively and qualitatively comparing PS4K and PS62K, it can be said that the differences in the decrease of the Young's modulus are due to their differences in their glass transition temperatures, which in turn are caused by the variation in their molecular weights.

The analogue of the Young's modulus for the plastically deformed region of PS4K and PS62K are shown in Fig. 5(b). It can be clearly seen that in case of PS62K there is practically no change in the analogue of the Young's modulus for plastic deformations with increasing temperature. The decrease in the analogue of Young's modulus for plastic deformations of PS62K is less than one order of magnitude for the entire experimental temperature range. In case of PS4K, there is almost three orders of magnitude decrease in the analogue of the Young's modulus for plastic deformations and this decrease is due to the lower value of T_g. The hardness of the sample decreases rapidly, when the polymer is heated above its glass transition temperature.

Determination of $E(T)$ or $E(v)$ provides a more detailed description of the elastic–plastic behaviour of the polymer rather than the mere determination of T_g, since the variation in the stiffness of the polymer at $T = T_g$ is not abrupt, but rather a gradual, continuous transition from the Young's modulus in the glassy state to the one in the rubbery state, as it can be seen in Fig. 5(a) and (b).

The determination of the elastic–plastic properties of the polymer as a function of temperature and frequency for the two polystyrene samples with different molecular weights has been made possible by the combination of the hyperbolic fit and TTS. Due to the limitations of the experimental set-up, it was not possible to attain higher temperatures in order to determine $E(T)$ or $E(v)$ in the rubbery plateau.

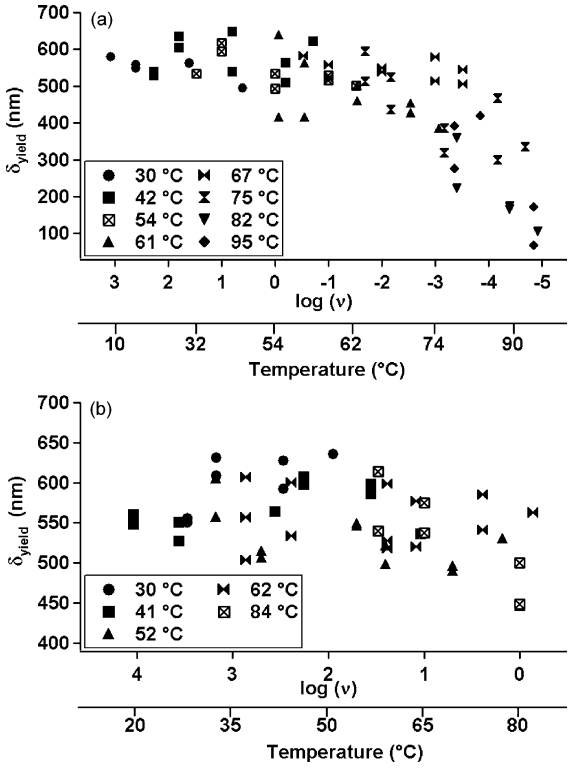

Fig. 6. Master curve of δ_{yield} as a function of $\log(v)$ of PS4K and PS62K obtained by shifting the isotherms with respect to reference temperature of 54 and 84 °C, respectively.

Fig. 6(a) shows the master curve of δ_{yield} as a function of frequency obtained for PS4K. For PS4K, the δ_{yield} is 600 nm around 10 °C (about 50 °C below T_g) and decreases to 66 nm around 97 °C (about 45 °C above T_g). In comparison the master curve of δ_{yield} for PS62K in Fig. 6(b) shows a very small decrease with increasing temperature. Only the measurement at 84 °C on PS62K shows a small decrease in the Young's modulus, in the analogue of Young's modulus for plastic deformations and in δ_{yield}, as the polymer approaches its T_g.

4. Conclusions

The most important result of this experiment is the ability to quantitatively and qualitatively characterise the temperature dependency of the Young's modulus of two polystyrene samples having different molecular weights and to compare them based on their differences in T_g, that in turn are due to the differences in molecular weight.

It has been shown that force–displacement curves are a powerful tool in order to determine the local viscoelastic properties of the polymer, such as Young's modulus and the yielding force, as a function of temperature and frequency. The difference in molecular masses, engendering differences in T_g, results in different temperature dependent viscoelastic properties of the two polystyrene samples. It has been possible to characterise this temperature dependent viscoelastic behaviour of the two polystyrene samples using a novel analysis technique.

For the first time, the shift coefficients of the isotherms of several mechanical properties have been fitted using both Arrhenius equation and WLF equation for low molecular weight polystyrene and Arrhenius equation for high molecular weight polystyrene. In case of low molecular weight polystyrene, the transition from Arrhenius equation fit to WLF equation fit has been shown and the intersection of the two fitting functions can be used to determine T_g. The C_1 and C_2 constants of the WLF equation and the activation energy determined from the Arrhenius equation are in very good agreement with the literature values.

In case of low molecular weight polystyrene, the Young's modulus, the analogue of Young's modulus for plastic deformations and the yielding force remains a constant till the temperature reaches T_g (57 °C) and then start to decrease rapidly. In case of high molecular weight polystyrene, all calculated quantities remain nearly a constant throughout the whole experiment, as T_g (97 °C) was higher than the maximum experimental temperature.

References

[1] Briscoe B, Fiori L, Pelillo E. J Phys D 1998;31:2395.
[2] Chizhik SA, Huang Z, Gorbunov VV, Myshkin NK, Tsukruk VV. Langmuir 1998;14:2606.
[3] Reynaud C, Sommer F, Quet C, El Bounia M, Duc TM. Surf Interface Anal 2000;30:185.
[4] Raghavan D, Gu X, Nguyen T, VanLandingham MR, Karim A. Macromolecules 2000;33:2573.
[5] Du B, Tsui OKC, Zhang Q, He T. Langmuir 2001;17:3286.
[6] Marti O, Stifter T, Waschipky H, Quintus M, Hild S. Colloids Surf A 1999;154:65.
[7] Tsui OKC, Wang XP, Ho JYL, Ng TK, Xiao X. Macromolecules 2000;33:4198.
[8] Bliznyuk VN, Assender HE, Briggs GAD. Macromolecules 2002;35:6613.
[9] Cappella B, Kaliappan SK, Sturm H. Macromolecules 2005;38:1874.
[10] Hertz H. J Reine Angew Math 1881;92:156.
[11] Peyser P. Glass transition temperature of polymers. In: Brandrup J, Immergut EH, editors. Polymer handbook. 3rd ed. New York: Wiley; 1989 [Chapter 6].
[12] Fox T, Flory P. J Polym Sci 1954;14:315.
[13] Domke J, Radmacher M. Langmuir 1998;14:3320.
[14] VanLandingham MR. Microsc Today 1997;97:12.
[15] Cappella B, Dietler G. Surf Sci Rep 1999;34:1.
[16] Tsukruk VV, Huang Z, Chizhik SA, Gorbunov VV. J Mater Sci 1998;99:4905.
[17] Du B, Tsui OKC, Zhang Q, He T. Langmuir 2001;17:3286.
[18] Cappella B, Sturm H, Schulz E. J Adhes Sci Technol 2002;16:921.
[19] Cappella B, Sturm H. J Appl Phys 2002;91:506.
[20] Munz M, Cappella B, Sturm H, Geuss M, Schulz E. Adv Polym Sci 2003;164:87.
[21] Maugis D. J Colloid Interface Sci 1992;150:243.
[22] Johnson KL, Greenwood JA. J Colloid Interface Sci 1997;192:326.
[23] Williams ML, Landel RF, Ferry JD. J Am Chem Soc 1955;77:3701.
[24] Fried JR. Sub-T_g transitions. In: Mark JE, editor. Physical properties of polymer handbook. New York: AIP Press; 1996 [Chapter 13].
[25] Chung CI, Sauer JA. J Polym Sci, Polym Phys 1971;9:1097.
[26] Tiller AR. Macromolecules 1992;25:4605.